

**Hidden-symmetry-protected quantum pseudo–spin Hall effect in optical lattices**Jing-Min Hou<sup>1,\*</sup> and Wei Chen<sup>2</sup><sup>1</sup>*Department of Physics, Southeast University, Nanjing 211189, China*<sup>2</sup>*College of Science, Nanjing University of Aeronautics and Astronautics, Nanjing 210016, China*

(Received 14 April 2016; published 20 June 2016)

We propose a scheme to realize a  $Z_2$  topological insulator in a square optical lattice. Different from the conventional topological insulator protected by the time-reversal symmetry, here the optical lattice possesses a hidden symmetry, which is responsible for the present  $Z_2$  topological order. With a properly defined pseudospin, such a topological insulator is characterized by the helical edge states that exhibits pseudo–spin-momentum locking, so it can be considered as a quantum pseudo–spin Hall insulator. The  $Z_2$  topological invariant is derived and its experimental detection is discussed as well.

DOI: [10.1103/PhysRevA.93.063626](https://doi.org/10.1103/PhysRevA.93.063626)**I. INTRODUCTION**

In recent decades, topological phases in condensed matter have attracted much attention [1,2]. Conventionally, it was thought that matter was classified according to symmetries based on Landau’s theory [3]. The discovery of the integer quantum Hall effect [4], which was first recognized to be related to topology, changed the viewpoint of physicists on the classification of matter [5]. The discovery of the time-reversal symmetry-protected topological insulators has stimulated more interest in the topological matter protected by symmetries [6–20]. Topological classification of matter is generally correlated with symmetries. Depending on the dimensionality and the symmetry classes specified by time-reversal symmetry and particle-hole symmetry, gapped systems can be classified into ten types of topological phases [21,22]. Besides the time-reversal and particle-hole symmetries, spatial symmetries, such as point symmetry, can protect a new kind of topological insulators, called topological crystalline insulators [23–25]. In previous work a hidden symmetry in a square lattice was found, which is responsible for the existence of the Dirac points [26]. This kind of hidden symmetry is a discrete antiunitary symmetry with a composite operator consisting of translation, complex conjugation, and sublattice exchange. A natural question is whether there exist topological insulators protected by such a hidden symmetry. In this paper we give an affirmative answer for this question and develop a kind of topological insulator protected by such a hidden symmetry.

The development of optical lattice and cold-atom techniques provides versatile models, some of which are hardly realized in solid real material. Therefore, cold atoms in optical lattices become a platform to explore various kinds of topological phases, especially those that are difficult to realize in real material. In recent years, many schemes have been proposed to realize various topological phases with neutral atoms in optical lattices. The the Harper Hamiltonian and effective magnetic fields have been experimentally realized [27–31]. Resorting to staggered effective magnetic fields, the quantum anomalous Hall effect was proposed to be realized in honeycomb lattices [32] and non-Abelian optical lattices

[33]. For the case with time-reversal symmetry, the quantum spin Hall effect was proposed to be realized with neutral atoms in optical lattices [34–37]. The schemes have also been designed to realize the time-reversal symmetry-protected three-dimensional topological insulators with neutral atoms in an optical lattice [37,38]. As a result, the mature techniques of cold atoms and optical lattices make it possible to realize the topological insulators protected by the hidden symmetry.

Here we propose a scheme of cold atoms in an optical lattice that preserves the hidden symmetry but breaks the time-reversal symmetry due to the existence of the hopping-accompanying phases. We find that this system supports the  $Z_2$  topological insulators protected by the hidden symmetry. In such an optical lattice, a pseudo-spin-operator can be defined, which has eigenvalues of  $\pm 1$ , corresponding to the pseudo-spin-up and pseudo-spin-down states. The pseudo-spin-up and pseudo-spin-down states are related by the hidden-symmetry operation. Therefore, we call the two-dimensional topological insulators quantum pseudo–spin Hall (QPSH) insulators. The edge states are helical, that is to say, the pseudo-spin-up and pseudo-spin-down states move along the opposite directions along the edge of the lattice, which is just the hallmark of the QPSH effect. We also define the hidden-symmetry polarization, which is an integer modulo 2, so that it is a  $Z_2$  topological invariant. The odd and even hidden-symmetry polarizations correspond to the QPSH insulator and the trivial band insulator, respectively. It should be pointed out that although the hidden symmetry plays a role in the QPSH effect like the time-reversal symmetry does in the quantum spin Hall effect, the hidden symmetry is distinct from the time-reversal symmetry. The hidden symmetry includes a translation operator, so the hidden-symmetry operator is momentum dependent in the concrete representation.

**II. MODEL**

Here we consider a two-component (two-color) system on a square lattice as shown in Fig. 1(a), where the arrows represent the hopping-accompanying phases. Due to the presence of these phases, the lattice is divided into two sublattices  $A$  and  $B$ . Each sublattice has the primitive lattice vectors  $\mathbf{a}_1 = (1, 1)$  and  $\mathbf{a}_2 = (1, -1)$ . In momentum space, the primitive reciprocal vectors are  $\mathbf{b}_1 = (\pi, \pi)$  and  $\mathbf{b}_2 = (\pi, -\pi)$ . The corresponding

\*jmh@seu.edu.cn

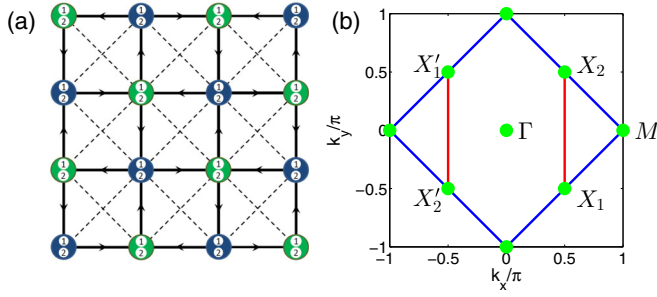


FIG. 1. (a) Schematic of the square optical lattices and the designed phase factor (denoted by arrows). Here the solid and dashed lines represent the nearest and next-nearest (diagonal) hopping, respectively; the green and blue circles represent the lattice sites of sublattices  $A$  and  $B$ , respectively; the numbers 1 and 2 in the circles denote the intrinsic atomic states. (b) The Brillouin zone, which is enclosed by the solid blue lines. Here the green solid circles represent the high-symmetry points. Along the red lines, the  $\Upsilon$  polarization is defined in the main text.

Brillouin zone is shown in Fig. 1(b). The tight-binding Hamiltonian can be written as  $H = H_0 + H_1 + H_2$ , with

$$H_0 = -t \sum_{i \in A} [e^{-i\gamma} a_i^\dagger (-i\tau_y) b_{i+\hat{x}} + e^{-i\gamma} a_i^\dagger (i\tau_y) b_{i-\hat{x}} + e^{i\gamma} a_i^\dagger (-i\tau_y) b_{i+\hat{y}} + e^{i\gamma} a_i^\dagger (i\tau_y) b_{i-\hat{y}} + \text{H.c.}], \quad (1)$$

$$H_1 = -t_1 \sum_{i \in A} [a_i^\dagger \tau_z a_{i+\hat{x}+\hat{y}} + a_i^\dagger \tau_z a_{i-\hat{x}-\hat{y}} + a_i^\dagger \tau_z a_{i-\hat{x}+\hat{y}} + a_i^\dagger \tau_z a_{i+\hat{x}-\hat{y}}] - t_1 \sum_{i \in B} [b_i^\dagger \tau_z b_{i+\hat{x}+\hat{y}} + b_i^\dagger \tau_z b_{i-\hat{x}-\hat{y}} + b_i^\dagger \tau_z b_{i-\hat{x}+\hat{y}} + b_i^\dagger \tau_z b_{i+\hat{x}-\hat{y}}], \quad (2)$$

and

$$H_2 = \lambda \sum_{i \in A} a_i^\dagger \tau_z a_i + \lambda \sum_{i \in B} b_i^\dagger \tau_z b_i, \quad (3)$$

where  $a_i = [a_i^{(1)}, a_i^{(2)}]^T$  and  $b_i = [b_i^{(1)}, b_i^{(2)}]^T$  are the two-component annihilation operators destructing a particle at a lattice site of sublattices  $A$  and  $B$ , respectively;  $\tau_i$  ( $i = x, y, z$ ) represents the Pauli matrices in the color space;  $t$  and  $t_1$  represent the amplitudes of hopping between the nearest lattice sites and between the next-nearest lattice sites, respectively;  $\lambda$  is an effective magnetic field; and  $0 < \gamma < \pi/2$  is a hopping-accompanying phase. Here the model can be realized by applying  ${}^6\text{Li}$  or  ${}^{40}\text{K}$  cold atoms trapped in an optical lattice. The color-switching hopping and the accompanying phases of hopping can be realized with laser-assisted tunneling techniques [29–31].

Taking the Fourier transformation on the Hamiltonian  $H$ , we rewrite it as  $H = [a_{\mathbf{k}}^{(1)\dagger}, a_{\mathbf{k}}^{(2)\dagger}, b_{\mathbf{k}}^{(1)\dagger}, b_{\mathbf{k}}^{(2)\dagger}] \mathcal{H}(\mathbf{k}) [a_{\mathbf{k}}^{(1)}, a_{\mathbf{k}}^{(2)}, b_{\mathbf{k}}^{(1)}, b_{\mathbf{k}}^{(2)}]^T$  with

$$\mathcal{H}(\mathbf{k}) = h_x(\mathbf{k})\sigma_x \otimes \tau_y + h_y(\mathbf{k})\sigma_y \otimes \tau_y + m(\mathbf{k})I \otimes \tau_z, \quad (4)$$

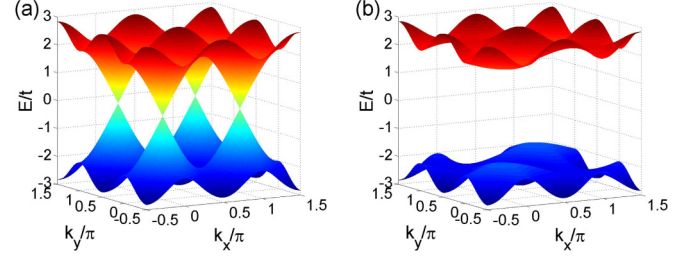


FIG. 2. Dispersion relation for (a)  $\gamma = \pi/4$ ,  $t_1 = 0$ , and  $\lambda = 0$  and (b)  $\gamma = \pi/4$ ,  $t_1 = 0.5t$ , and  $\lambda = 0.3t$ .

where  $h_x(\mathbf{k}) = -2t \cos \gamma (\sin k_x + \sin k_y)$  and  $h_y(\mathbf{k}) = -2t \sin \gamma (\sin k_x - \sin k_y)$ ;  $m(\mathbf{k}) = (\lambda - 4t_1 \cos k_x \cos k_y)$  is the mass term;  $\sigma_{x,y}$  represent the Pauli matrices in the sublattice space. The dispersion relation is  $E(\mathbf{k})_{\pm} = \pm \sqrt{h_x(\mathbf{k})^2 + h_y(\mathbf{k})^2 + m(\mathbf{k})^2}$ , which is shown in Fig. 2. For this system, there are four bands and the valence and conduction bands are twofold degenerate. When the diagonal hopping terms  $H_1$  and the effective magnetic terms  $H_2$  are absent, the mass term in the Bloch Hamiltonian (4) vanishes. The corresponding dispersion relation is shown in Fig. 2(a), from which one finds that the Dirac points occur at the points  $\Gamma$  and  $M$  in the Brillouin zone. When the diagonal hopping terms  $H_1$  and the effective magnetic terms  $H_2$  are present, a gap opens as shown in Fig. 2(b) and then the system turns into an insulator.

### III. HIDDEN SYMMETRY

It is easy to verify that the total system  $H$  preserves a hidden symmetry, i.e.,  $[H, \Upsilon] = 0$ , with the symmetry operator  $\Upsilon$  defined as

$$\Upsilon = (\sigma_x \otimes I) K T_{\hat{x}}, \quad (5)$$

where  $T_{\hat{x}}$  is a translation operator that moves the lattice by  $\hat{x}$  along the  $x$  direction,  $K$  is the complex conjugation operator,  $\sigma_x$  is the Pauli matrix representing the sublattice exchange, and  $I$  is the unit matrix in the color space. For the Bloch Hamiltonian, the corresponding transformation can be described by

$$\Upsilon \mathcal{H}(\mathbf{k}) \Upsilon^{-1} = \mathcal{H}(-\mathbf{k}). \quad (6)$$

Therefore, for each energy band, there always exists another energy band corresponding to the  $\Upsilon$  transformed quantum states. These two energy bands comprise a pair of bands related to each other by the hidden symmetry  $\Upsilon$ , which are referred to as the  $\Upsilon$  pair bands. The Bloch function is supposed to have the form  $\Psi_{\mathbf{k}}(\mathbf{r}) = [u_{A,\mathbf{k}}^{(1)}(\mathbf{r}), u_{A,\mathbf{k}}^{(2)}(\mathbf{r}), u_{B,\mathbf{k}}^{(1)}(\mathbf{r}), u_{B,\mathbf{k}}^{(2)}(\mathbf{r})]^T e^{i\mathbf{k}\cdot\mathbf{r}}$  in the coordinate representation. The symmetry operator  $\Upsilon$  acts on the Bloch function as follows:

$$\Upsilon \Psi_{\mathbf{k}}(\mathbf{r}) = \begin{pmatrix} u_{B,\mathbf{k}}^{(1)*}(\mathbf{r} - \hat{x}) e^{i\mathbf{k}\cdot\mathbf{r}} \\ u_{B,\mathbf{k}}^{(2)*}(\mathbf{r} - \hat{x}) e^{i\mathbf{k}\cdot\mathbf{r}} \\ u_{A,\mathbf{k}}^{(1)*}(\mathbf{r} - \hat{x}) e^{i\mathbf{k}\cdot\mathbf{r}} \\ u_{A,\mathbf{k}}^{(2)*}(\mathbf{r} - \hat{x}) e^{i\mathbf{k}\cdot\mathbf{r}} \end{pmatrix} e^{-i\mathbf{k}\cdot\mathbf{r}} = \Psi'_{\mathbf{k}}(\mathbf{r}). \quad (7)$$

Because  $\Upsilon$  is the symmetry operator of the system,  $\Psi'_{\mathbf{k}}(\mathbf{r})$  must be a Bloch wave function of the system. Thus,

we obtain  $\mathbf{k}' = -\mathbf{k}$ ,  $u_{A,\mathbf{k}'}^{(i)}(\mathbf{r}) = u_{B,\mathbf{k}}^{(i)*}(\mathbf{r} - \hat{x})e^{ik_x}$ , and  $u_{B,\mathbf{k}'}^{(i)}(\mathbf{r}) = u_{A,\mathbf{k}}^{(i)*}(\mathbf{r} - \hat{x})e^{ik_x}$  with  $i = 1, 2$ . From Eq. (7) it is easy to show that the operator  $\Upsilon$  has the effect when acting on wave vectors as  $\Upsilon : \mathbf{k} \rightarrow -\mathbf{k} = \mathbf{k}'$ . If  $\mathbf{k}' = \mathbf{k} + \mathbf{G}$ , where  $\mathbf{G}$  is the reciprocal lattice vector, then we can say that  $\mathbf{k}$  is an  $\Upsilon$ -invariant point in momentum space. We find four distinct  $\Upsilon$ -invariant points in the Brillouin zone as

$$\Gamma = (0,0), \quad M = (\pi,0), \quad X_{1,2} = (\pi/2, \pm \pi/2). \quad (8)$$

For the hidden-symmetry operator  $\Upsilon$ , we have  $\Upsilon^2 = T_{2\hat{x}}$ , which has the representation based on the Bloch wave functions as  $\Upsilon^2 = e^{-i2\mathbf{k}\cdot\hat{x}}$ . Thus, we have  $\Upsilon^2 = -1$  at the  $\Upsilon$ -invariant points  $X_{1,2}$  while  $\Upsilon^2 = 1$  at  $\Gamma$  and  $M$ . Since  $\Upsilon$  is an antiunitary operator, it is straightforward to show that  $\Upsilon$ -protected degeneracy must occur at the points  $X_{1,2}$  [26].

#### IV. QUANTUM PSEUDO-SPIN HALL EFFECT

We define an operator as

$$S = \sigma_z \otimes \tau_z, \quad (9)$$

which has two eigenvalues  $\xi = \pm 1$ . Thus, the operator  $S$  can be considered as a pseudo-spin-operator. It is easy to verify that the pseudo-spin-operator  $S$  commutes with the Bloch Hamiltonian (4), i.e.,  $[\mathcal{H}(\mathbf{k}), S] = 0$ , so the Bloch Hamiltonian and the pseudo-spin-operator have common eigenstates. That is to say, every Bloch wave function can have a fixed eigenvalue of  $S$  with  $+1$  or  $-1$ .

When the gap opens, there exist two kinds of insulators, which are topologically distinct. When the system turns from one kind of insulator into the other, a topological phase transition happens. We can manifest this scenario with band inversions.

When the mass term  $m(\mathbf{k})$  is absent, the energy bands have two distinct Dirac points at  $\Gamma$  and  $M$  in the Brillouin zone. Around the Dirac points, the Bloch Hamiltonian can be linearized in the form

$$\mathcal{H}_{\Gamma,M}(\mathbf{k}) = \sum_{ij} v_{ij}^{\Gamma,M} p_i \sigma_j \otimes \tau_y, \quad (10)$$

with

$$v^\Gamma = \begin{pmatrix} -2t \cos \gamma & -2t \sin \gamma \\ -2t \cos \gamma & 2t \sin \gamma \end{pmatrix} \quad (11)$$

and

$$v^M = \begin{pmatrix} 2t \cos \gamma & 2t \sin \gamma \\ -2t \cos \gamma & 2t \sin \gamma \end{pmatrix}, \quad (12)$$

where  $\mathbf{p}$  is the relative wave vector from the Dirac points. About the Dirac points, we find  $w = \text{sgn}(\det[v^{\Gamma,M}]) = \pm 1$ , which has opposite values for the two distinct Dirac points at  $\Gamma$  and  $M$ .

As we mentioned above, when the diagonal hopping terms  $H_1$  and the effective magnetic terms  $H_2$  are present, a gap opens and the system turns into an insulator for the half-filling case. We can find that the mass terms in the Bloch Hamiltonian have different signs in different parameter ranges. There are four cases: (i) When  $\lambda - 4t_1 > 0$  and  $\lambda + 4t_1 > 0$ , the mass terms at two Dirac points are both positive; (ii) when  $\lambda - 4t_1 < 0$  and  $\lambda + 4t_1 < 0$ , the mass terms at two Dirac points are both

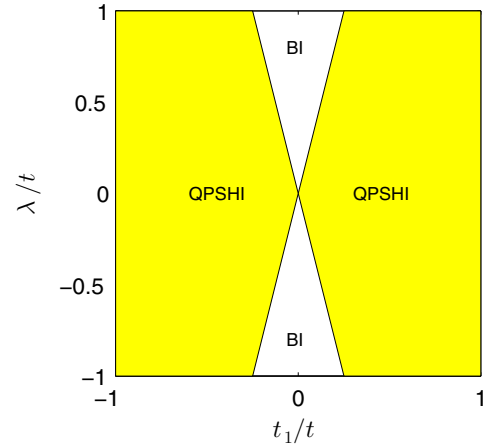


FIG. 3. Phase diagram. Here QPSHI and BI denote quantum pseudo-spin Hall insulators and conventional band insulators, respectively.

negative; (iii) when  $\lambda - 4t_1 < 0$  and  $\lambda + 4t_1 > 0$ , the mass at the  $\Gamma$  point is negative and the one at the  $M$  point remains positive; (iv) when  $\lambda - 4t_1 > 0$  and  $\lambda + 4t_1 < 0$  are satisfied, the mass at the  $\Gamma$  point is positive and the one at the  $M$  point is negative. For cases (i) and (ii) the mass terms at points  $\Gamma$  and  $M$  have the same sign and the system is a conventional band insulator. In contrast, for cases (iii) and (iv) they have opposite signs and the system is a topological insulator. The conventional band insulators and topological insulators can be distinguished by the edge states. When the mass terms at one of the points change sign, a band inversion happens, which implies that a topological phase transition occurs. Based on the signs of the mass terms at the Dirac points  $\Gamma$  and  $M$ , we obtain the phase diagram as shown in Fig. 3.

We obtain the edge states by diagonalizing the Hamiltonian of a strip geometry. The dispersion relations of a strip geometry are shown in Fig. 4. For the parameter ranges in cases (i) and (ii) there are no edge states, as shown in Figs. 4(a) and 4(b), which confirms that the parameters in cases (i) and (ii) correspond to the conventional band insulators. For parameter ranges in cases (iii) and (iv) there is a pair of helical edge states at each surface transversing the band gap, as shown in Figs. 4(c) and 4(d), which indicates the existence of topological insulators.

We find that the edge states  $|\psi_{\pm,k_x}\rangle$  of the strip geometry are eigenstates of the operator  $S = \sigma_z \otimes \tau_z$  with the eigenvalue  $\xi = \pm 1$ , i.e.,  $S|\psi_{\pm,k_x}\rangle = \pm|\psi_{\pm,k_x}\rangle$ . It is easy to verify that the operator  $S$  anticommutes with the hidden-symmetry operator  $\Upsilon$ , i.e.,  $[S, \Upsilon]_+ = 0$ , so we have

$$\Upsilon|\psi_{\xi,k_x}\rangle = e^{i\alpha}|\psi_{-\xi,-k_x}\rangle, \quad (13)$$

where  $\alpha$  is a phase depending on the gauge. That is to say, the particles in different edge states on the same boundary move in the opposite direction with different eigenvalues of  $S$ . We can consider the operator  $S$  as the pseudo-spin-operator. Thus, the edge states are pseudo-spin-momentum locking. The fact that the edge states are related by the hidden-symmetry operator  $\Upsilon$  is solid evidence that the edge states are protected by the hidden symmetry  $\Upsilon$ .

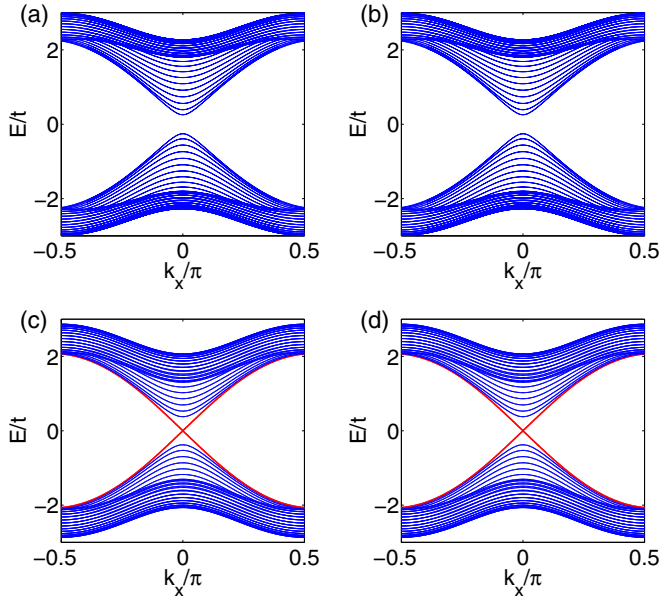


FIG. 4. Dispersion relations of a strip geometry for (a) case (i) with  $t_1 = 0.2t$  and  $\lambda = t$ , (b) case (ii) with  $t_1 = -0.2t$  and  $\lambda = -t$ , (c) case (iii) with  $t_1 = 0.2t$  and  $\lambda = 0.5t$ , and (d) case (iv) with  $t_1 = -0.2t$  and  $\lambda = -0.5t$ .

## V. THE $Z_2$ TOPOLOGICAL INVARIANT

It is well known that the time-reversal symmetry can lead to the existence of the  $Z_2$  two-dimensional topological insulators, i.e., the quantum spin Hall insulators. The system considered here preserves a hidden symmetry, which is also a discrete antiunitary symmetry. Similar to the time-reversal symmetry leading to the quantum spin Hall insulators, the hidden symmetry can also lead to a kind of  $Z_2$  topological insulator. Similar to the definition of time-reversal polarization for the time-reversal symmetry-protected spin quantum Hall insulator [14,39], we can define the  $\Upsilon$  polarization for the insulators preserving the  $\Upsilon$  symmetry.

The Bloch wave-function occupied band can be written as  $|\Psi_{n,\mathbf{k}}\rangle = e^{i\mathbf{k}\cdot\mathbf{r}}|u_{n,\mathbf{k}}\rangle$ , where  $|u_{n,\mathbf{k}}\rangle$  is the cell-periodic eigenstate of the Bloch Hamiltonian  $\mathcal{H}(\mathbf{k})$ . The Berry connection matrix

$$\mathbf{a}_{mn} = -i\langle u_{m,\mathbf{k}}|\nabla_{\mathbf{k}}|u_{n,\mathbf{k}}\rangle. \quad (14)$$

For the hidden symmetry  $\Upsilon$ , we define a matrix as

$$w_{mn}(\mathbf{k}) = \langle u_{m,-\mathbf{k}}|\Upsilon|u_{n,\mathbf{k}}\rangle, \quad (15)$$

which is antisymmetric at the  $\Upsilon$ -invariant degenerate points  $X_{1,2}$ .

For the present model with half filling, there are two occupied bands, which comprise the  $\Upsilon$  pair bands. For the occupied  $\Upsilon$  pair bands we can define the charge polarization in terms of the Berry connection along a direction in the Brillouin zone [see red lines in Fig. 1(b)] as

$$P_\rho = \frac{1}{2\pi} \left[ \int_{X_1}^{X_2} \mathbf{A}(\mathbf{k}) \cdot d\mathbf{k} + \int_{X'_1}^{X'_2} \mathbf{A}(\mathbf{k}) \cdot d\mathbf{k} \right], \quad (16)$$

where  $\mathbf{A}(\mathbf{k})$  is defined as  $\text{tr}[\mathbf{a}(\mathbf{k})]$ . For each occupied band, the partial charge polarization is defined as

$$P_i = \frac{1}{2\pi} \left[ \int_{X_1}^{X_2} \mathbf{a}_{ii}(\mathbf{k}) \cdot d\mathbf{k} + \int_{X'_1}^{X'_2} \mathbf{a}_{ii}(\mathbf{k}) \cdot d\mathbf{k} \right]. \quad (17)$$

For the  $\Upsilon$  pair bands, we can also define the  $\Upsilon$  polarization as

$$\begin{aligned} P_\Upsilon &= P_1 - P_2 = 2P_1 - P_\rho \\ &= \frac{1}{2\pi} \int_{X_1}^{X_2} [\mathbf{A}(\mathbf{k}) - \mathbf{A}(-\mathbf{k})] \cdot d\mathbf{k} - \frac{i}{\pi} \ln \frac{w_{12}(X_2)}{w_{12}(X_1)} \\ &= \frac{1}{i\pi} \ln \left[ \frac{\sqrt{w_{12}(X_1)^2}}{w_{12}(X_1)} \cdot \frac{w_{12}(X_2)}{\sqrt{w_{12}(X_2)^2}} \right], \end{aligned} \quad (18)$$

which is an integer and only defined modulo 2 due to the ambiguity of the logarithm. The argument of the logarithm has only two values  $\pm 1$  associated with the even and odd values of  $P_\Upsilon$ , respectively. Therefore, we can rewrite Eq. (18) as

$$(-1)^{P_\Upsilon} = \prod_{i=1}^2 \frac{\text{Pf}[w(X_i)]}{\sqrt{\det[w(X_i)]}}. \quad (19)$$

The  $Z_2$  topological invariant can be defined as  $P_\Upsilon$  modulo 2. When  $P_\Upsilon$  is odd or even, the system is a topological insulator or a trivial band insulator. Equation (19) gives a distinct definition of the  $Z_2$  topological invariant. However, evaluating the  $Z_2$  topological invariant with Eq. (19) requires a continuous gauge from the point  $X_1$  to the  $X_2$  in the Brillouin zone, which is a difficult task for numerical calculations. Fortunately, the  $Z_2$  topological invariant can be obtained by calculating the Berry gauge potential and the Berry curvature proposed by Fukui and Hatsugai [40] or by evaluating the non-Abelian Berry connection derived from the Wannier function center proposed by Yu *et al.* [41].

## VI. TECHNIQUES FOR EXPERIMENTAL DETECTION OF THE $Z_2$ TOPOLOGICAL INVARIANT

Conventionally, the topological invariants in solid materials are detected by measuring the transport properties. However, this method is infeasible for cold atomic systems. Thus, other methods to identify topological insulators have been proposed and even performed experimentally. One method is to detect edge states by Bragg spectroscopy [42] or direct imaging [43]. Important progress in measuring the topological invariant is the experimental realization of directly measuring the Zak phase by using a combination of Bloch oscillations with Ramsey interferometry [44]. Based on the same experimental techniques, a scheme has been designed to measure the Chern number in two-dimensional lattices [45]. Later, the scheme was generalized to detect  $Z_2$  topological invariants based on the same experimental techniques [46]. Therefore, these methods can also be applied to detect the topological order in the quantum pseudo-spin Hall insulator in our study.

## VII. CONCLUSION

In summary, we have proposed a scheme to realize a  $Z_2$  topological insulator in a square optical lattice. Such a non-

trivial topological phase is protected by the hidden-symmetry  $\Upsilon$  that is a composite antiunitary symmetry consisting of translation, complex conjugation, and sublattice exchange. The hidden symmetry is intrinsically different from time-reversal symmetry. Because of the inclusion of the translation operation, the hidden symmetry is momentum dependent in a specific representation and there are only two degenerate symmetry-invariant points in the two-dimensional Brillouin zone instead of four degenerate symmetry-invariant points as in the case of time-reversal symmetry. Based on the hidden symmetry, the pseudospin was defined and the  $Z_2$  topological invariant was derived, for which the new topological insulator was dubbed a quantum pseudo-spin Hall insulator. Through numerical calculations, helical edge states were found for the nontrivial topological phase. Helical edge states are pseudo-spin-momentum locking and two edge states moving in opposite directions form  $\Upsilon$  pairs, which is solid evidence

of the new  $Z_2$  topological insulator being protected by the hidden symmetry  $\Upsilon$ . The detection of the  $Z_2$  topological invariant through the techniques of cold atoms and optical lattices was also discussed. Our work opens a perspective to search for new classes of topological phases by studying the hidden symmetries of the lattices.

#### ACKNOWLEDGMENTS

J.-M.H. acknowledges support from the National Natural Science Foundation of China under Grant No. 11274061. W.C. acknowledges support from the National Natural Science Foundation of China under Grant No. 11504171, the National Science Foundation of Jiangsu Province, China under Grant No. BK20150734, and the Project funded by China Postdoctoral Science Foundation under Grants No. 2014M560419 and No. 2015T80544.

- 
- [1] M. Z. Hasan and C. L. Kane, *Rev. Mod. Phys.* **82**, 3045 (2010).
  - [2] X. L. Qi and S. C. Zhang, *Rev. Mod. Phys.* **83**, 1057 (2011).
  - [3] L. D. Landau, *Phys. Z. Sowjetunion* **11**, 26 (1937).
  - [4] K. von Klitzing, G. Dorda, and M. Pepper, *Phys. Rev. Lett.* **45**, 494 (1980).
  - [5] D. J. Thouless, M. Kohmoto, M. P. Nightingale, and M. den Nijs, *Phys. Rev. Lett.* **49**, 405 (1982).
  - [6] C. L. Kane and E. J. Mele, *Phys. Rev. Lett.* **95**, 226801 (2005).
  - [7] C. L. Kane and E. J. Mele, *Phys. Rev. Lett.* **95**, 146802 (2005).
  - [8] B. A. Bernevig and S. C. Zhang, *Phys. Rev. Lett.* **96**, 106802 (2006).
  - [9] B. A. Bernevig, T. L. Hughes, and S. C. Zhang, *Science* **314**, 1757 (2006).
  - [10] M. König, S. Wiedmann, C. Brüne, A. Roth, H. Buhmann, L. W. Molenkamp, X. L. Qi, and S. C. Zhang, *Science* **318**, 766 (2007).
  - [11] L. Fu, C. L. Kane, and E. J. Mele, *Phys. Rev. Lett.* **98**, 106803 (2007).
  - [12] J. E. Moore and L. Balents, *Phys. Rev. B* **75**, 121306 (2007).
  - [13] R. Roy, *Phys. Rev. B* **79**, 195322 (2009).
  - [14] L. Fu and C. L. Kane, *Phys. Rev. B* **76**, 045302 (2007).
  - [15] D. Hsieh, D. Qian, L. Wray, Y. Xia, Y. S. Hor, R. J. Cava, and M. Z. Hasan, *Nature (London)* **452**, 970 (2008).
  - [16] Y. Xia, D. Qian, D. Hsieh, L. Wray, A. Pal, H. Lin, A. Bansil, D. Grauer, Y. S. Hor, R. J. Cava, and M. Z. Hasan, *Nat. Phys.* **5**, 398 (2009).
  - [17] H. Zhang, C. X. Liu, X. L. Qi, X. Dai, Z. Fang, and S. C. Zhang, *Nat. Phys.* **5**, 438 (2009).
  - [18] Y. L. Chen *et al.*, *Science* **325**, 178 (2009).
  - [19] D. Hsieh *et al.*, *Nature (London)* **460**, 1101 (2009).
  - [20] D. Hsieh, Y. Xia, D. Qian, L. Wray, F. Meier, J. H. Dil, J. Osterwalder, L. Patthey, A. V. Fedorov, H. Lin, A. Bansil, D. Grauer, Y. S. Hor, R. J. Cava, and M. Z. Hasan, *Phys. Rev. Lett.* **103**, 146401 (2009).
  - [21] A. P. Schnyder, S. Ryu, A. Furusaki, and A. W. W. Ludwig, *Phys. Rev. B* **78**, 195125 (2008); in *Advances in Theoretical Physics: Landau Memorial Conference*, edited by V. Lebedev and M. Feigel'man, AIP Conf. Proc. No. 1134 (AIP, New York, 2009), p. 10.
  - [22] A. Kitaev, in *Advances in Theoretical Physics: Landau Memorial Conference* (Ref. [21]), p. 22.
  - [23] L. Fu, *Phys. Rev. Lett.* **106**, 106802 (2011).
  - [24] T. H. Hsieh, H. Lin, J. Liu, W. Duan, A. Bansil, and L. Fu, *Nat. Commun.* **3**, 982 (2012).
  - [25] C. X. Liu, R. X. Zhang, and B. K. VanLeeuwen, *Phys. Rev. B* **90**, 085304 (2014).
  - [26] J. M. Hou, *Phys. Rev. Lett.* **111**, 130403 (2013).
  - [27] H. Miyake, G. A. Siviloglou, C. J. Kennedy, W. C. Burton, and W. Ketterle, *Phys. Rev. Lett.* **111**, 185302 (2013).
  - [28] M. Aidelsburger, M. Atala, M. Lohse, J. T. Barreiro, B. Paredes, and I. Bloch, *Phys. Rev. Lett.* **111**, 185301 (2013).
  - [29] M. Aidelsburger, M. Atala, S. Nascimbéne, S. Trotzky, Y.-A. Chen, and I. Bloch, *Phys. Rev. Lett.* **107**, 255301 (2011).
  - [30] J. Struck, C. Ölschläger, M. Weinberg, P. Hauke, J. Simonet, A. Eckardt, M. Lewenstein, K. Sengstock, and P. Windpassinger, *Phys. Rev. Lett.* **108**, 225304 (2012).
  - [31] J. Struck, M. Weinberg, C. Ölschläger, P. Windpassinger, J. Simonet, K. Sengstock, R. Höppner, P. Hauke, A. Eckardt, M. Lewenstein, and L. Mathey, *Nat. Phys.* **9**, 738 (2013).
  - [32] L. B. Shao, S. L. Zhu, L. Sheng, D. Y. Xing, and Z. D. Wang, *Phys. Rev. Lett.* **101**, 246810 (2008).
  - [33] N. Goldman, A. Kubasiak, A. Bermudez, P. Gaspard, M. Lewenstein, and M. A. Martin-Delgado, *Phys. Rev. Lett.* **103**, 035301 (2009).
  - [34] N. Goldman, I. Satija, P. Nikolic, A. Bermudez, M. A. Martin-Delgado, M. Lewenstein, and I. B. Spielman, *Phys. Rev. Lett.* **105**, 255302 (2010).
  - [35] G. Liu, S. L. Zhu, S. Jiang, F. Sun, and W. M. Liu, *Phys. Rev. A* **82**, 053605 (2010).
  - [36] C. J. Kennedy, G. A. Siviloglou, H. Miyake, W. C. Burton, and W. Ketterle, *Phys. Rev. Lett.* **111**, 225301 (2013).
  - [37] B. Béri and N. R. Cooper, *Phys. Rev. Lett.* **107**, 145301 (2011).
  - [38] A. Bermudez, L. Mazza, M. Rizzi, N. Goldman, M. Lewenstein, and M. A. Martin-Delgado, *Phys. Rev. Lett.* **105**, 190404 (2010).
  - [39] L. Fu and C. L. Kane, *Phys. Rev. B* **74**, 195312 (2006).
  - [40] T. Fukui and Y. Hatsugai, *J. Phys. Soc. Jpn.* **76**, 053702 (2007).

- [41] R. Yu, X. L. Qi, A. Bernevig, Z. Fang, and X. Dai, *Phys. Rev. B* **84**, 075119 (2011).
- [42] N. Goldman, J. Beugnon, and F. Gerbier, *Phys. Rev. Lett.* **108**, 255303 (2012).
- [43] N. Goldman, J. Dalibard, A. Dauphin, F. Gerbier, M. Lewenstein, P. Zoller, and I. B. Spielman, *Proc. Natl. Acad. Sci. USA* **110**, 6736 (2013).
- [44] M. Atala, M. Aidelsburger, J. T. Barreiro, D. Abanian, T. Kitagawa, E. Demler, and I. Bloch, *Nat. Phys.* **9**, 795 (2013).
- [45] D. A. Abanin, T. Kitagawa, I. Bloch, and E. Demler, *Phys. Rev. Lett.* **110**, 165304 (2013).
- [46] F. Grusdt, D. Abanin, and E. Demler, *Phys. Rev. A* **89**, 043621 (2014).